Critical-Point Structure in Photoelectric Emission Energy Distributions

EVAN O. KANE
Bell Telephone Laboratories, Murray Hill, New Jersey 07971
(Received 17 June 1968)

Structure in photoelectric energy distributions is analyzed on the basis of a model which assumes that the electrons are created in the volume by direct transitions, and ignores lifetime broadening and the distortion of the distribution function due to the escape probability. In this model, the structure consists of square edges and logarithmically infinite peaks due to two-dimensional critical points where the optical energy surface is tangent to the electron energy surface. As the photon energy is varied the loci of these critical points trace out "critical lines" in k space. A plot of the electron energy of the structure versus photon energy is called the "E-ω image" of the critical line. Simple properties of these lines and their images are derived and illustrated by explicit calculations for the band structure of silicon. The critical lines pass through the three-dimensional critical points of the electron energy function (ECP) and those of the optical energy function (OCP). An ECP and an OCP will coincide when required to by symmetry, and are then called symmetry critical points (SCP). ECP's are extrema of $E(\hbar\omega)$ along critical lines, while OCP's are extrema of $\hbar\omega(E)$. E-ω images will "kink" or intersect at SCP's. The "strength" of critical-point structure varies rapidly along critical lines and tends to infinity as an SCP is approached. These properties should be useful in inferring energy-band information from experimental plots of E-ω images. They will also be helpful in analyzing machine calculations of photoelectric energy distributions.

I. INTRODUCTION AND CONCLUSIONS

PHOTOELECTRIC energy distributions have been extensively used as a means of studying the energy-band structure of solids.[1–4] In some materials a model of indirect transitions appears to be applicable,[1,2] in which case peaks in the one-electron density of states in either the valence or conduction band are readily inferred. In materials for which the model of direct transitions is a good approximation, structure is also to be expected. The interpretation in this case is more complex but potentially richer in information content, provided lifetime-broadening and energy-loss processes are not too large.

In the "direct-transitions" model, with exciton effects ignored, the carriers created by the light lie on an "optical energy shell" or surface in k space whose equation is

$$\hbar\omega = \mathcal{E}_i(\mathbf{k}) - \mathcal{E}_j(\mathbf{k}), \tag{1}$$

where $\mathcal{E}_j(\mathbf{k})$ is the energy of the initial state and $\mathcal{E}_i(\mathbf{k})$ is the energy of the final state. The photon energy is $\hbar\omega$ and its momentum has been ignored. The electron energy $\mathcal{E}_i(\mathbf{k})$ is a variable function over the two-dimensional space of the optical energy shell and possesses van Hove singularities[5,6] or critical points in its energy distribution. Geometrically, these critical points occur where the electron energy surface and the optical energy surface are tangent. The tangencies may be of extremal type (the electron energy is a local minimum or a maximum at such a point) or of saddle-point type where the relative curvatures have opposite signs in the two principal directions. Characteristic of two dimensions, a van Hove singularity leads to a "square-edge" discontinuity in the electron energy distribution function for an extremal critical point and to a logarithmic singularity for the saddle-point case. We use the subscripts s, u, l to denote saddle, upper (maximal energy), and lower (minimal energy) critical points.

As the photon energy varies, the locus of a two-dimensional critical point traces out a line in k space which we refer to as a "critical line." In Sec. II we discuss some simple topological properties of critical lines. We prove that critical lines cannot "kink" or terminate at "ordinary points," i.e., points of no special symmetry in k space. Two critical lines will not intersect at an ordinary point.

In addition to the critical lines or two-dimensional critical points, the three-dimensional critical points of the electron energy function $\mathcal{E}_i(\mathbf{k})$ and of the optical energy function $\mathcal{E}_i(\mathbf{k})-\mathcal{E}_j(\mathbf{k})$ are also of importance.[6] We call these ECP and OCP, respectively. An ECP and an OCP will only coincide when it is required by symmetry, in which case we call it a symmetry critical point (SCP).

We prove that every ECP and OCP which is not an SCP has one and only one critical line running through it. We prove that an analytic SCP may have up to three critical lines intersecting it. Nonanalytic SCP appear to offer the possibility of still larger numbers of critical-line intersections but we have not studied this case.

The strength of a two-dimensional critical point may be defined as the amplitude of discontinuity in the extremal case or as the coefficient of the logarithmic singularity in the saddle-point case. Expressions for the strength are derived and it is shown that the strength tends to infinity as an SCP is reached. It may also tend to infinity at a general point with an attendant change of type, from s to u or s to l or the reverse.

[1] W. E. Spicer, Phys. Rev. Letters **11**, 243 (1963).
[2] C. N. Berglund and W. E. Spicer, Phys. Rev. **136**, A1030 (1964); **136**, A1044 (1964).
[3] A. J. Blodgett and W. E. Spicer, Phys. Rev. **158**, 514 (1967).
[4] R. C. Eden and W. E. Spicer (to be published).
[5] L. van Hove, Phys. Rev. **89**, 1189 (1953).
[6] D. Brust, Phys. Rev. **134**, A1337 (1964).

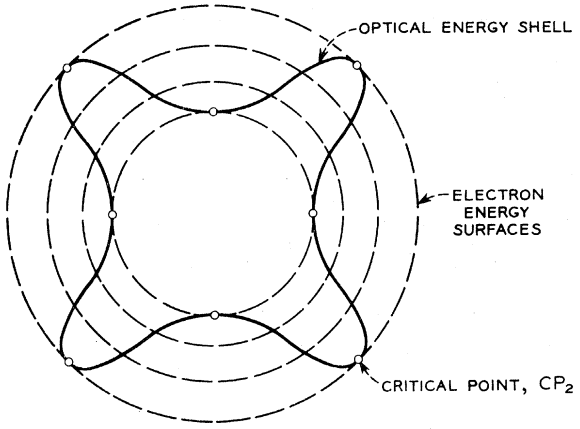

FIG. 1. Optical energy shell, solid line, for fixed photon energy $\hbar\omega$. The dashed lines are surfaces of constant electron energy. Points of tangency between optical and electron energy surfaces give critical points CP_2 indicated by open dots.

To make contact with experiment, we discuss the E-ω images of critical lines. These are electron versus photon energy plots along critical lines or, experimentally, plots of peak or edge structure in electron energy distributions versus photon energy. The intersection of two E-ω lines does not imply the intersection of the corresponding critical lines but an intersection of three or more lines would give evidence of critical-line intersections and hence imply that the intersection was a symmetry critical point, SCP. ECP's and OCP's imply extrema in the functions $E(\omega)$ and $\omega(E)$, respectively. The converse need not be true. These properties should be useful in using E-ω plots either to interpret theoretical energy-distribution calculations or to infer band-structure information from experiment.

In Sec. III we calculate electron energy and optical energy contours in the (110) plane for silicon. We also calculate critical lines and critical points, ECP's and OCP's. We compute the singularity strength along the critical lines and plot the E-ω images of some of the stronger critical lines.

Brust[7] has used E-ω plots to analyze his theoretical calculations of energy distributions and finds agreement with several of the conspicuous critical lines we have identified. Higher-resolution theoretical calculations would undoubtedly turn up more structure and increase the certainty of identification.

Our calculations all refer to the "internal yield" $d\tilde{y}/dE$. The external yield dy/dE may be found by convoluting $d\tilde{y}/dE$ with an escape function $P(E,E')$ [2,8]:

$$\frac{dy}{dE}=\int P(E,E')\frac{d\tilde{y}}{dE'}dE'. \tag{2}$$

In the case of cesium-covered silicon in the photon energy range studied by Allen and Gobeli[9] the escape function appears to provide considerable distortion of $d\tilde{y}/dE$ and even to introduce additional structure.[8] Such distortion will be most severe at low electron energies where the phonon mean free path is short compared to the mean free path for pair production. The recent studies of Callcott[10] and Eden and Spicer[4] at higher photon energies should be freer of distortion due to $P(E,E')$ and should provide more accurate band-structure information. Theoretical calculations of the energy distributions at higher photon energies currently in progress[11] should aid in the interpretation of the experimental results.

II. STRUCTURE IN PHOTOELECTRIC ENERGY DISTRIBUTIONS DUE TO CRITICAL POINTS AND CRITICAL LINES

We assume that we are dealing with photoelectrons which are produced in the volume of a semiconductor by direct optical excitation. The absorptive part of the dielectric constant ϵ_2 is given by[6]

$$\epsilon_2(\omega)=A\sum_{i,j}\int_{\mathrm{BZ}}d\mathbf{k}\,|\mathbf{p}_{ij}(\mathbf{k})|^2\delta(\hbar\omega-\mathcal{E}_i(\mathbf{k})+\mathcal{E}_j(\mathbf{k})), \tag{3}$$

$$A=e^2/6\pi m_0^2\omega^2V.$$

The sum is over all conduction bands i and valence bands j. $\mathbf{p}_{ij}$ is the momentum matrix element between bands. The δ function is for energy conservation. The assumption of direct transitions and neglect of the momentum of the light leads to the same value of $\mathbf{k}$ in both bands i and j. The spin is supposed to be considered in the sum of i, j.

The δ function in Eq. (3) leads to the result that the electrons produced by direct transitions lie on an "optical energy shell" whose equation is given in (1). The optical energy shell is a "weighted" surface or "shell" with a weighting factor

$$|\mathbf{p}_{ij}(\mathbf{k})|^2|\nabla_k[\mathcal{E}_i(\mathbf{k})-\mathcal{E}_j(\mathbf{k})]|^{-1}.$$

When we refer to the "shell area" we mean the surface area with this weighting factor.

We define an internal quantum-differential yield $d\tilde{y}/dE$ by the equation

$$\frac{d\tilde{y}}{dE}=A\sum_{i,j}\int_{\mathrm{BZ}}d\mathbf{k}\,|\mathbf{p}_{ij}(\mathbf{k})|^2\delta(\hbar\omega-\mathcal{E}_i(\mathbf{k})+\mathcal{E}_j(\mathbf{k}))\times\delta(E-\mathcal{E}_i(\mathbf{k}))/\epsilon_2. \tag{4}$$

The internal yield $d\tilde{y}/dE$ is just the energy distribution of the electrons as they are created. Since we are interested in the yield per absorbed quantum, we have divided by ϵ_2. The use of Eqs. (3) and (4) shows that

[7] D. Brust, Phys. Rev. **139**, A489 (1965).
[8] E. O. Kane, J. Phys. Soc. Japan Suppl. **21**, 37 (1966).
[9] F. G. Allen and G. W. Gobeli, Phys. Rev. **144**, 558 (1966).
[10] T. A. Callcott, Phys. Rev. **161**, 746 (1967).
[11] D. Brust (private communication).

$d\tilde{y}/dE$ has unit normalization

$$\int \frac{d\tilde{y}}{dE} dE = 1. \tag{5}$$

The geometric construction equivalent to Eq. (4) is shown in Fig. 1. The solid curve is the optical energy shell and the dashed curves are electron energy shells. The quantity $(d\tilde{y}/dE)\Delta E$ is the weighted area of the optical energy shell lying between the electron energy surfaces $\mathcal{E}_i(k)=E$ and $\mathcal{E}_i(k)=E+\Delta E$. The electron density of states $\rho(E)$ is given by

$$\rho(E)=\frac{1}{(2\pi)^3}\sum_i \int_{\mathrm{BZ}} d\mathbf{k}\,\delta(E-\mathcal{E}_i(\mathbf{k})). \tag{6}$$

We will confine our analysis to analytic points of energy versus $\mathbf{k}$ vector. We then write $\mathcal{E}(\mathbf{k})$ as a power series to second order in $\mathbf{k}-\mathbf{k}_0$, where $\mathbf{k}_0$ is some given point and $\mathbf{k}$ is in its neighborhood.

$$\mathcal{E}_i(\mathbf{k})=e_i+\boldsymbol{\alpha}^{(i)}\cdot(\mathbf{k}-\mathbf{k}_0)+(\mathbf{k}-\mathbf{k}_0)\cdot\boldsymbol{\beta}^{(i)}\cdot(\mathbf{k}-\mathbf{k}_0). \tag{7}$$

$\boldsymbol{\beta}$ is proportional to the reciprocal effective-mass tensor. We also want to consider optical energy bands, $\mathcal{E}_i(\mathbf{k})-\mathcal{E}_j(\mathbf{k})$, which, of course, have expansions analogous to Eq. (7) with the definitions

$$\begin{aligned}\mathcal{E}_i(\mathbf{k})-\mathcal{E}_j(\mathbf{k})&=e_{ij}+\boldsymbol{\alpha}^{(ij)}\cdot(\mathbf{k}-\mathbf{k}_0)\\&\quad+(\mathbf{k}-\mathbf{k}_0)\cdot\boldsymbol{\beta}^{(ij)}\cdot(\mathbf{k}-\mathbf{k}_0),\\ e_{ij}&\equiv e_i-e_j,\\ \boldsymbol{\alpha}^{(ij)}&\equiv\boldsymbol{\alpha}^{(i)}-\boldsymbol{\alpha}^{(j)},\\ \boldsymbol{\beta}^{(ij)}&\equiv\boldsymbol{\beta}^{(i)}-\boldsymbol{\beta}^{(j)}.\end{aligned} \tag{8}$$

A. Critical Points

A critical point is defined as a point where $\boldsymbol{\alpha}=0$. In the case $\boldsymbol{\alpha}^{(ij)}(\mathbf{k}_0)=0$, we call $\mathbf{k}_0$ an optical critical point, OCP. If $\boldsymbol{\alpha}^{(i)}(\mathbf{k}_0)=0$, $\mathbf{k}_0$ is called an energy critical point, ECP. If $\mathbf{k}_0$ is a point of high symmetry, the condition $\boldsymbol{\alpha}=0$ may be required by symmetry. In this case (and, we assume, only in this case) $\mathbf{k}_0$ will be simultaneously an OCP and an ECP. We use the special name, symmetry critical point, SCP, for this case. The SCP's will have a special importance in the theory of critical lines to be developed in Sec. II B.

The importance of the three-dimensional critical points, OCP and ECP, in yielding structure in reflectivity and the density of states is very well known.[6,12] In order to contrast with the two-dimensional results we give a brief review.

There are four types of three-dimensional critical points (or van Hove singularities) labeled M_i, $i=0, 1, 2, 3$, where the index i is the number of negative β coefficients (the tensor is assumed diagonal) in Eq. (7) or (8). All four types yield square-root-type structure in ϵ_2 versus $\hbar\omega$ or ρ versus E.[6] A simple graph of ϵ_2 versus $\hbar\omega$ is given in Fig. 2 illustrating the appearance of the four types of singularity.[6] Equation (7) may be used to give $\delta\rho$, the contribution to ρ from the vicinity of the critical points in the analytic form:

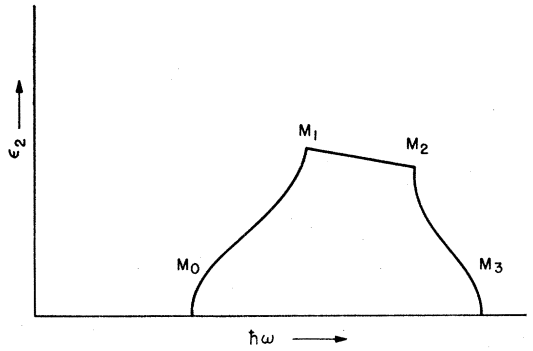

FIG. 2. Structure in the optical density of states ϵ_2 versus energy $\hbar\omega$ resulting from optical critical points (OCP). The subscripts give the number of negative mass coefficients.

for extremal points M_0 and M_3:

$$\delta\rho=S_E[\epsilon(E-e_i)]^{1/2}, \quad \epsilon(E-e_i)>0 \tag{9}$$

$$\delta\rho=0, \quad \epsilon(E-e_i)<0; \tag{10}$$

for saddle points M_1 and M_2:

$$\delta\rho=a-S_E[\epsilon(E-e_i)]^{1/2}, \quad \epsilon(E-e_i)>0 \tag{11}$$

$$\delta\rho=a+b(E-e_i), \quad \epsilon(E-e_i)<0 \tag{12}$$

$$S_E\equiv 2\pi/\tilde{\beta}^{3/2}, \tag{13}$$

$$\tilde{\beta}\equiv|\beta_{11}{}^i\beta_{22}{}^i\beta_{33}{}^i|^{1/3}, \tag{14}$$

$$\epsilon\equiv\beta_{11}{}^i/|\beta_{11}{}^i|. \tag{15}$$

The axes have been defined so that β_{22} and β_{33} have the same sign. $\boldsymbol{\beta}$ is assumed diagonal. In the saddle-point case, some cutoff must be assumed to limit the contribution to $\delta\rho$ to the vicinity of $\mathbf{k}_0$. The constants a and b in (11) and (12) depend on the choice of cutoff but the strength S_E of the nonanalytic contribution does not. The saddle points M_1 and M_2 appear to be more prominent than the extremal points M_0 and M_3 in Fig. 2. Equations (9) and (11) indicate that all four types will be equally prominent in the energy derivative. This is one of the advantages of derivative methods in studying critical points.[13]

B. Critical Lines

We now discuss the structure of the internal differential yield $d\tilde{y}/dE$ in Eq. (4), using Eqs. (7) and (8).

[12] J. C. Phillips, J. Phys. Chem. Solids **12**, 208 (1960); J. C. Phillips, in *Solid State Physics*, edited by F. Seitz and D. Turnbull (Academic Press Inc., New York, 1966), Vol. 18, p. 55.

[13] B. O. Seraphin and R. B. Hess, Phys. Rev. Letters **14**, 138 (1965); M. Cardona, K. L. Shaklee, and F. H. Pollak, Phys. Rev. **154**, 696 (1967); W. E. Engeler, M. Garfinkel, J. J. Tiemann, and H. Fritzsche, Phys. Rev. Letters **14**, 1069 (1965); G. W. Gobeli and E. O. Kane, *ibid.* **15**, 142 (1965); I. Balslev, Phys. Rev. **143**, 636 (1966).

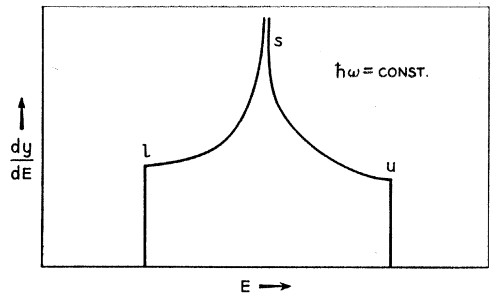

FIG. 3. Structure in the internal energy distribution function $d\tilde{y}/dE$ versus E, for photoelectrons produced by light of frequency $\hbar\omega$, is shown due to critical points CP_2 or "critical lines." l, s, u denote the critical-point-type classification as lower extremum, saddle point, and upper extremum, respectively.

As we have remarked previously, electrons created by direct transitions lie on an optical energy surface in $\mathbf{k}$ space given by Eq. (1) and illustrated in Fig. 1. $d\tilde{y}/dE$ is the energy-distribution function of the electrons as they are created on this surface. In the first part of our discussion, we think of $\hbar\omega$ as fixed so that we concentrate on the two-dimensional space of the optical energy surface. Just as before, we find that in this space there are "ordinary points" and "critical points." The critical points lead to structure in $d\tilde{y}/dE$ in the same way that the OCP of Sec. II A lead to structure in plots of ϵ_2 versus $\hbar\omega$.[6,12] We will sometimes call these points CP_2, the subscript 2 referring to the two-dimensional energy surface on which they lie. When $\hbar\omega$ is allowed to vary, the locus of the CP_2 trace out lines in k space. We will usually refer to the CP_2 as "critical lines."

An "ordinary point" in this discussion is one where $\boldsymbol{\alpha}^{(i)}$ and $\boldsymbol{\alpha}^{(j)}$ are *not* parallel. Linear terms in the expansion of Eqs. (7) and (8) are then sufficient. Axes may be chosen such that

$$\mathcal{E}_i(\mathbf{k})-\mathcal{E}_j(\mathbf{k})=e_{ij}+\alpha_1^{(ij)}(k_1-k_{01}), \tag{16}$$

$$\mathcal{E}_i(\mathbf{k})=e_i+\alpha_1^{(i)}(k_1-k_{01})+\alpha_2^{(i)}(k_2-k_{02}). \tag{17}$$

With the use of Eqs. (16) and (17) in Eq. (4) it is easy to integrate over the δ functions and obtain

$$\frac{d\tilde{y}}{dE}=\sum_{i,j}\frac{1}{\alpha_1^{(ij)}\alpha_2^{(i)}\epsilon_2}\int dk_3|\mathbf{p}_{ij}(\mathbf{k})|^2, \tag{18}$$

$$\hbar\omega=\mathcal{E}_i(\mathbf{k})-\mathcal{E}_j(\mathbf{k}), \tag{19}$$

$$E=\mathcal{E}_i(\mathbf{k}). \tag{20}$$

Equations (19) and (20) define an "optical energy surface" and a "constant energy surface," respectively. The variable k_3 in Eq. (18) runs over the line of intersection of these two surfaces. When the two surfaces are tangent, their normals are parallel, $\boldsymbol{\alpha}^{(i)}$ parallel to $\boldsymbol{\alpha}^{(ij)}$. $\alpha_2^{(i)}$ is then equal to zero by construction and we have a critical point, CP_2. These critical points are shown as circles in Fig. 1.

At a critical point we need to include quadratic terms from Eqs. (7) and (8). We integrate over k_1 as before, eliminating the "optical energy δ function" and installing Eq. (19). We then use Eqs. (19) and (16) to eliminate the k_1 degree of freedom and obtain

$$\frac{d\tilde{y}}{dE}=\sum_{i,j}\frac{1}{\alpha_1^{(ij)}}\int dk_2dk_3|p_{ij}(\mathbf{k})|^2\delta\Big[E-\frac{\alpha_1^{(i)}}{\alpha_1^{(ij)}}(\hbar\omega-\hbar\omega_0)+\alpha_1^{(i)}\{\gamma_2(k_2-k_{02})^2+\gamma_3(k_3-k_{03})^2\}\Big], \tag{21}$$

$$\sum_{l=2}^{3}\gamma_l(k_l-k_{0l})^2=\sum_{l,m=2}^{3}\left(\frac{\beta_{lm}^{(i)}}{\alpha_1^{(i)}}-\frac{\beta_{lm}^{(ij)}}{\alpha_1^{(ij)}}\right)\times(k_l'-k_{0l}')\cdot(k_m'-k_{0m}'). \tag{22}$$

The γ's are related to the β/α's by a transformation of axes to diagonal form indicated by Eq. (22). The γ's are the relative curvatures of the optical energy and electron energy surfaces. Equation (21) is then integrated to give for the extremal point

$$\delta\left(\frac{d\tilde{y}}{dE}\right)=S_L, \quad \alpha_1^{(i)}\gamma_2(E-E_0)>0$$
$$=0, \quad \alpha_1^{(i)}\gamma_2(E-E_0)<0 \tag{23}$$

and for the saddle point

$$\delta\left(\frac{d\tilde{y}}{dE}\right)=a-\frac{S_L}{\pi}\ln|E-E_0|, \tag{24}$$

$$S_L=\pi|\mathbf{p}_{ij}(\mathbf{k}_0)|^2/\alpha_1^{(ij)}\alpha_1^{(i)}\bar{\gamma}, \tag{25}$$

$$\bar{\gamma}=(\gamma_2\gamma_3)^{1/2}. \tag{26}$$

The constant a depends on the assumed cutoff.

We note that again we have two types of critical points depending on whether optical and electron energy surfaces have an extremal or saddle type of tangency. In the extremal case, the differential yield is constant with energy and falls abruptly to zero at E_0 when the surfaces separate. The saddle-point case gives a logarithmic infinity at the critical point so that this type of singularity tends to be more prominent. Figure 3 shows the structure in the energy-distribution curves due to critical points CP_2. l, u, and s denote lower- and upper-extrema and saddle-type CP_2, respectively. The sharp corners and spikes will become rounded when lifetime broadening is considered.

The saddle-type CP_2 are more prominent than the extremal CP_2, as was also the case for OCP and ECP. To enhance the extremal structure, a further derivative may be taken. In a plot of $d^2\tilde{y}/dE^2$ the extremal points would also give infinite peaks in the absence of lifetime broadening.

It is worth noting that the strength coefficient S_L in Eq. (25) does not have a singularity for $\alpha_1^{(i)}=0$, or $\alpha_1^{(ij)}=0$ separately. This is easily seen using Eq. (22).

This means that ECP's and OCP's do not strongly enhance the structure in $d\tilde{y}/dE$. Of course, when $\alpha_1^{(i)}=\alpha_1^{(ij)}=0$ simultaneously, S_L will be singular. This occurs when an ECP and an OCP coincide, as they must at certain points of high symmetry. We have called such points SCP's. The enhancement of the structure due to critical lines which occurs at an SCP may be useful as a tool for identifying SCP's.

Using Eq. (21), we note that the type of CP_2, l, u, or s is determined by the signs of $\alpha_1^{(i)}\gamma_2$ and $\alpha_1^{(i)}\gamma_3$.

C. Properties of Critical Lines

In deriving some simple but useful properties of critical lines we first discuss solutions of the equation

$$r\boldsymbol{\alpha}=\boldsymbol{\beta}\cdot\mathbf{x}, \tag{27}$$

with $\boldsymbol{\alpha}$ a nonzero vector, $\boldsymbol{\beta}$ a diagonalizable tensor, $\mathbf{x}$ an unknown vector, and r a variable scalar. Without loss of generality we choose the coordinate system for which $\boldsymbol{\beta}$ is diagonal and rewrite Eq. (27):

$$r\alpha_l=\beta_{ll}x_l, \quad l=1, 2, 3. \tag{28}$$

These equations *always* possess a nonzero solution for some r. For all $\beta_{ll}\neq 0$, the solutions form a single straight line as r takes on all values. If one, and only one, $\beta_{ii}=0$, $\alpha_i\neq 0$, we must take $r=0$ and the solutions are the straight line $x_{j\neq i}=0$, x_i unrestricted. If $\beta_{ii}=\alpha_i=0$ or if two or more β_{ii} are zero the solutions will cover a plane or all of three dimensions.

In studying the properties of critical lines we use the Taylor-series expansion of Eqs. (7) and (8) for all bands. We study three cases successively, namely, where $\mathbf{k}_0$, the origin of the expansion, is a CP_2, an OCP or ECP, and an SCP.

1. $\mathbf{k}_0$ *is a* CP_2

The condition that a general point $\mathbf{k}$ be a CP_2 is

$$\nabla_{\mathbf{k}}\mathcal{E}_i(\mathbf{k})=r\nabla_{\mathbf{k}}\{\mathcal{E}_i(\mathbf{k})-\mathcal{E}_j(\mathbf{k})\}, \tag{29}$$

where r is any scalar. With the help of Eqs. (7) and (8) we write (29) in the vicinity of $\mathbf{k}_0$:

$$\boldsymbol{\alpha}^{(i)}+\boldsymbol{\beta}^{(i)}\cdot(\mathbf{k}-\mathbf{k}_0)=r\{\boldsymbol{\alpha}^{(ij)}+\boldsymbol{\beta}^{(ij)}\cdot(\mathbf{k}-\mathbf{k}_0)\}. \tag{30}$$

We use the fact that $\mathbf{k}_0$ is a CP_2. Let r_0 be the value of r in Eq. (30) for $\mathbf{k}=\mathbf{k}_0$. Write $r=r_0+\delta r$. Treating $\mathbf{k}-\mathbf{k}_0$ and δr as first-order infinitesimals, we write Eq. (30) to first order as

$$\delta r\boldsymbol{\alpha}^{(ij)}=\{\boldsymbol{\beta}^{(i)}-r_0\boldsymbol{\beta}^{(ij)}\}\cdot(\mathbf{k}-\mathbf{k}_0). \tag{31}$$

Equation (31) is now of the form of Eq. (27). Using the properties derived above, we can immediately write down the theorem:

(i) A critical line cannot end on an analytic point.

This follows since Eq. (31) always possesses solutions along a line through $\mathbf{k}_0$.

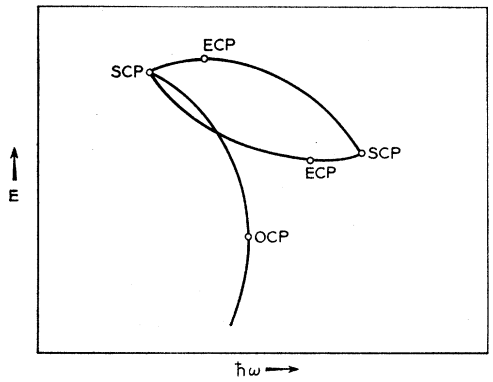

FIG. 4. E-ω images of critical lines. Electron energy is plotted versus photon energy along critical lines. Critical points OCP, ECP, and SCP are indicated by open dots.

We can also state the following statement or theorem.

(ii) It is highly improbable for two critical lines to intersect at a point of low symmetry.

This holds since we have seen that the solution of Eq. (27) is generally only a *single* line. In order to have two or more lines intersecting at $\mathbf{k}_0$ we must satisfy at least two conditions. Either $\beta_{ii}=\alpha_i=0$ or $\beta_{ii}=\beta_{jj\neq ii}=0$. (When these conditions are met a degenerate planar solution results. The use of higher-order terms in the power series would be required to resolve the degeneracy.) Since there is only one degree of freedom along a critical line we cannot expect to satisfy two conditions simultaneously unless one or more of them is required by symmetry.[14]

To give an example where symmetry permits critical-line intersections, consider the (100) line in a cubic crystal. This is a critical line by symmetry. The components of $\boldsymbol{\alpha}$ normal to (100) are zero by symmetry. Since we have one degree of freedom along the (100) line, we can expect to satisfy $\beta_{ii}=0$ for some point, where i refers to a direction normal to (100). Another critical line may intersect the (100) line at such a point, and we have found instances in silicon where this occurs in practice. (See Fig. 14.)

2. $\mathbf{k}_0$ *is an OCP or an ECP*

We discuss the case for an ECP but the case for an OCP is entirely analogous. At an ECP, Eq. (30) becomes

$$\boldsymbol{\beta}^{(i)}\cdot(\mathbf{k}-\mathbf{k}_0)=r\{\boldsymbol{\alpha}^{(ij)}+\boldsymbol{\beta}^{(ij)}\cdot(\mathbf{k}-\mathbf{k}_0)\}. \tag{32}$$

Treating $(\mathbf{k}-\mathbf{k}_0)$ as a first-order infinitesimal, we see that r is a first-order infinitesimal, hence we neglect the second term on the right of Eq. (32) as being of higher order and obtain

$$\boldsymbol{\beta}^{(i)}\cdot(\mathbf{k}-\mathbf{k}_0)=r\boldsymbol{\alpha}^{(ij)}. \tag{33}$$

[14] We say "highly improbably" rather than "vanishingly improbable" since we have not examined this point in the rigorous manner of Herring. See C. Herring, Phys. Rev. **52**, 363 (1937).

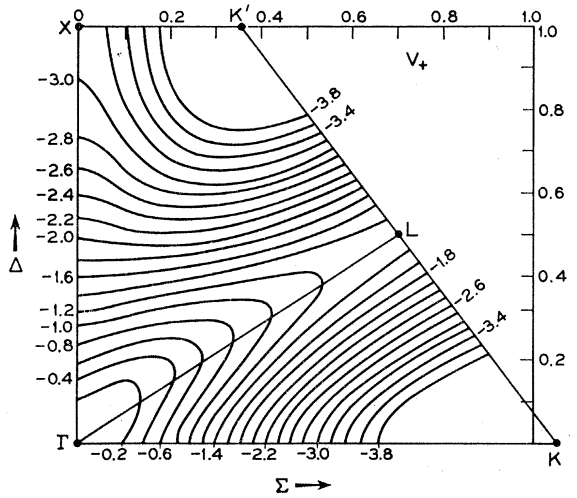

FIG. 5. Highest positive-parity valence band V_+. Contours of constant electron energy for silicon in the (110) plane. Contour lines are separated by 0.2 eV. The valence-band maximum is the energy zero.

Equation (33) is of the same form as Eq. (27), hence we may conclude:

(iii) Every critical point, ECP or OCP, has one, and only one, critical line passing through it.

The question of two or more critical lines intersecting at $\mathbf{k}_0$ is the same as in Sec. II C *1*. Since here $\mathbf{k}_0$ is a point, there are no degrees of freedom with which to satisfy the conditions required for intersecting lines.

3. $\mathbf{k}_0$ *is an Analytic SCP*

Here Eq. (30) becomes

$$\beta^{(i)}\cdot(\mathbf{k}-\mathbf{k}_0)=r\beta^{(ij)}\cdot(\mathbf{k}-\mathbf{k}_0). \tag{34}$$

If $\beta^{(ij)}$ has all nonzero eigenvalues, it will possess an inverse $\{\beta^{(ij)}\}^{-1}$. Multiplying Eq. (34) through by this inverse, we have

$$\begin{aligned}\beta'\cdot(\mathbf{k}-\mathbf{k}_0)&=r(\mathbf{k}-\mathbf{k}_0),\\ \beta'&\equiv\{\beta^{(ij)-1}\cdot\beta^{(i)}\}.\end{aligned} \tag{35}$$

Although $\beta^{(i)}$ and $\beta^{(ij)}$ are always Hermitian, β' is Hermitian if, and only, if $\beta^{(i)}$ and $\beta^{(ij)}$ commute, i.e., if they have the same principal axes. Hermiticity of β' will be guaranteed if the symmetry of the point $\mathbf{k}_0$ is high enough. If β' is Hermitian, there are three real solutions and three corresponding orthogonal critical lines intersecting at $\mathbf{k}_0$.

If $\mathbf{k}_0$ is a nonanalytic SCP, the equation analogous to Eq. (34) which determines the critical lines in the vicinity of $\mathbf{k}_0$ is of higher algebraic order. Hence a nonanalytic SCP will generally permit more than three critical lines to intersect at $\mathbf{k}_0$.

4. *E-ω Images of Critical Lines*

In order to make contact with experiment we wish to consider a plot of electron energy versus photon energy along critical lines. If structure in experimental dy/dE versus E plots is due to critical lines, then an experimental plot of peak and edge energies versus photon energy $\hbar\omega$ should correspond to the theoretical plots of E versus $\hbar\omega$ along critical lines. We now derive a few simple properties of these plots which we call E-ω images of critical lines.

Let s be the length as measured along a critical line. Since we have shown these lines to be "unkinked" except possibly at nonanalytic points of $\mathcal{E}(\mathbf{k})$ or at SCP's, we expect $\mathcal{E}_i(s)$ and $\hbar\omega(s)=\mathcal{E}_i(s)-\mathcal{E}_j(s)$ to be analytic functions of the variable s. If $d\mathcal{E}_i/ds\neq 0$, the parameter s can be eliminated to give $\hbar\omega(\mathcal{E}_i)$ as an analytic function. If $d\hbar\omega/ds\neq 0$, we can write $\mathcal{E}_i(\hbar\omega)$ as an analytic function. Because of the one-dimensional character of the lines, we do not expect to simultaneously satisfy $d\hbar\omega/ds=d\mathcal{E}_i/ds=0$ except when symmetry requires it. At such symmetry points we have

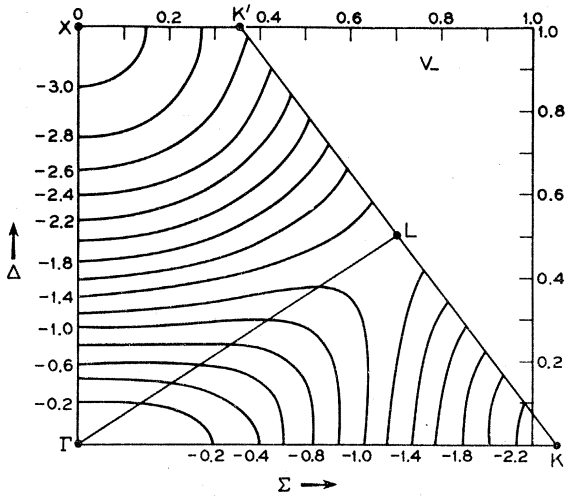

FIG. 6. Highest negative-parity valence band V_-. Contours of constant electron energy for silicon in the (110) plane. Contour lines are separated by 0.2 eV. The valence-band maximum is the energy zero.

$$\begin{aligned}\mathcal{E}_i&=\epsilon_i+\beta_i s^2,\\ \hbar\omega&=\epsilon_{ij}+\beta_{ij}s^2.\end{aligned} \tag{36}$$

Hence we see that the $E(\hbar\omega)$ contours actually terminate (or kink) at $E=\epsilon_i$, $\hbar\omega=\epsilon_{ij}$ since s^2 cannot be negative. Hence the E-ω image lines will terminate only at points whose $\mathbf{k}$ counterimage has special symmetry. Such points will frequently be SCP's. However, when an ordinary critical line in $\mathbf{k}$ space intersects a symmetry critical line this will also cause the E-ω image of the ordinary critical line to terminate.

If two critical lines intersect in $\mathbf{k}$ space their E-ω images must also intersect but the reverse will usually

not be true. However, if more than two E-ω images intersect simultaneously or if an E-ω image terminates or is kinked, this is an indication that the $\mathbf{k}$ counterimage has some special symmetry, the most likely situation being that $\mathbf{k}$ is an SCP.

Another desirable aspect of an SCP is that it causes the strength of the critical structure to tend to infinity, as we have noted previously. (The singularity remains integrable so that, with lifetime broadening, a finite peak or edge results.) This means that structure becomes more prominent just where peaks are coalescing or kinking or otherwise indicating that the $\mathbf{k}$ counterimage has special symmetry.

Other interesting features of the E-ω images are their extrema. An ECP will lead to an extremum of $E(\hbar\omega)$ whereas an OCP will lead to an extremum of $\hbar\omega(E)$. The converse is not necessarily true.

These points are illustrated schematically in Fig. 4. E-ω image lines are shown terminating or kinking at SCP's. The extrema in E versus ω are shown as ECP's and the extremum in ω versus E is shown as an OCP.

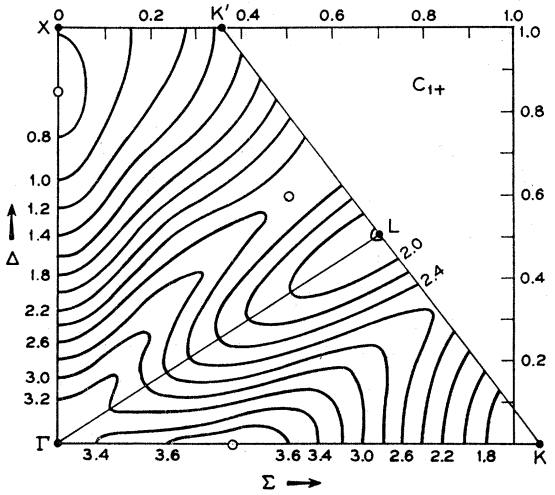

FIG. 7. Lowest positive-parity conduction band C_{1+}. Contours of constant electron energy for silicon in the (110) plane. Contour lines are separated by 0.2 eV. The valence-band maximum is the energy zero. Circles are critical points, ECP.

III. APPLICATION TO SILICON BAND STRUCTURE

In this section we illustrate some of the generalities of the preceding sections with the use of a model band calculation, namely, the empirical pseudopotential approximation to silicon as given by Brust, Cohen, and Phillips.[6,15] We follow their model and calculational procedure exactly. We represent the potential by the three parameters:

$$V_{111}=-0.21, \quad V_{220}=0.04, \quad V_{311}=0.08, \quad (37)$$

where the energies are in rydbergs.

[15] D. Brust, M. L. Cohen, and J. C. Phillips, Phys. Rev. Letters 9, 389 (1962).

We have diagonalized exactly the interactions between all plane waves whose kinetic energy at the point $\mathbf{k}$ was less than 35 eV. We treated by second-order perturbation theory interactions with all bands of energy greater than 35 eV whose kinetic energy at $\mathbf{k}=0$ was less or equal 85 eV. These perturbation interactions were incorporated in the Hamiltonian prior to diagonalization in the manner of Brust[6] and Löwdin.[16]

We have not made a complete calculation of all critical points and lines in the entire zone. Our investigation has been restricted to the (110) plane. We chose this plane because it contains the important symmetry directions [100], [111], and [110]. Also, the (110) is itself a reflection plane. Because of reflection symmetry, all energy surfaces intersect the (110) plane normally. Thus one of the conditions for an OCP, ECP, or a critical line is automatically satisfied. We may then expect that a great many critical points and critical lines will lie in the (110) plane.

We have not made a more complete survey of critical lines partly because of the labor involved and partly because we feel that a critical-line analysis is not an adequate substitute for a direct calculation of $d\tilde{y}/dE$. To be sure, the strengths of all the critical lines are easily computed, but we find that there are a large number of critical lines and we have no accurate way of adding them all together.

The critical-line analysis should be helpful in interpreting a more straightforward calculation of $d\tilde{y}/dE$ as to what parts of $\mathbf{k}$ space contribute to the more important features. Since the calculated critical lines suggest that a great deal of structure is actually present, the straightforward calculation may have to be done with considerable accuracy in order to resolve the structure clearly.

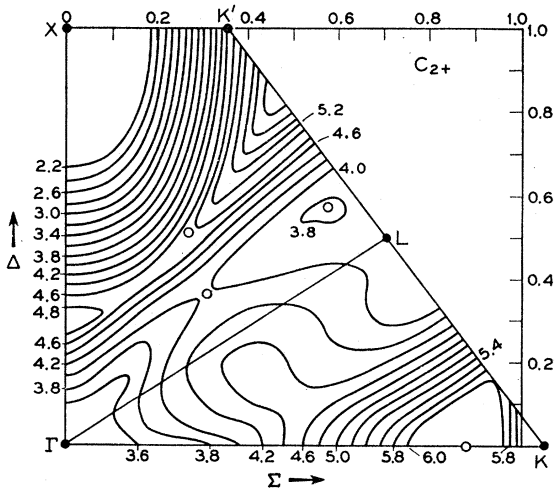

FIG. 8. Second-lowest positive-parity conduction band C_{2+}. Contours of constant electron energy for silicon in the (110) plane. Contour lines are separated by 0.2 eV. The valence-band maximum is the energy zero. Circles are critical points, ECP.

[16] P. Löwdin, J. Chem. Phys. 19, 1396 (1951).

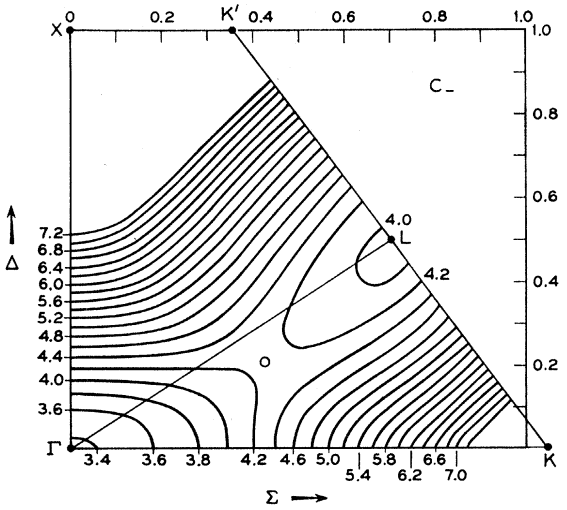

FIG. 9. Lowest negative-parity conduction band C_-. Contours of constant electron energy for silicon in the (110) plane. Contour lines are separated by 0.2 eV. The valence-band maximum is the energy zero. Circles are critical points, ECP.

The first high-resolution numerical studies of critical-point structure were made for phonon spectra by Gilat and Raubenheimer.[17] More recently their technique has been successfully applied to electron energy bands in silicon by Saravia and Brust.[18] It is to be hoped that

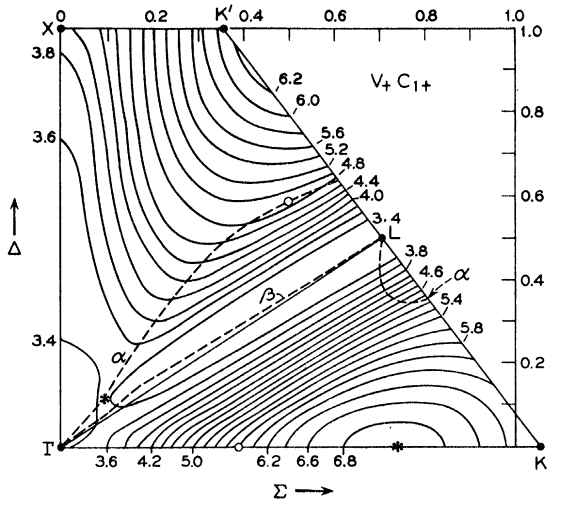

FIG. 10. Optical energy band; transition V_+ to C_{1+}. Contours of constant photon energy for silicon in the (110) plane. Contour lines are separated by 0.2 eV. Dashed lines are critical lines denoted by Greek letters. Stars are critical points, OCP. Circles are conduction-band ECP.

these high-resolution methods will soon be applied to the more computationally difficult problem of calculating photoelectric energy distributions.

[17] G. Gilat and L. J. Raubenheimer, Phys. Rev. **147**, 670 (1966); **144**, 390 (1966).

[18] L. R. Saravia and D. Bru t, Phys. Rev. **171**, 916 (1968).

In our analysis, the electron energy bands have been calculated and classified according to their signature or "reflection parity" under reflection in the (110) plane. This classification is meaningful only in the plane itself. It was done because the bands so defined have simple analytic properties. If the bands are classified according to energy ordering, crossing singularities occur. For example, the entire [111] direction

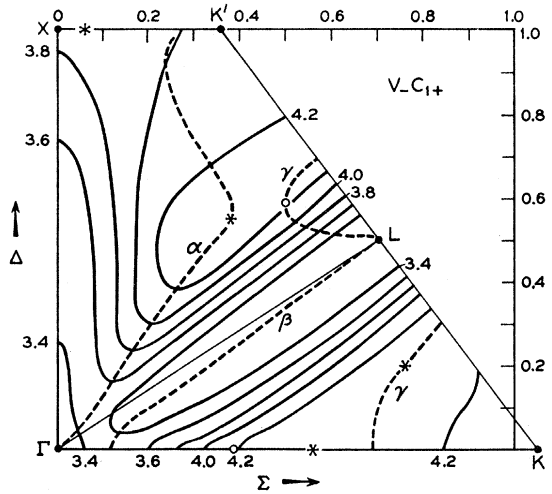

FIG. 11. Optical energy band; transition V_- to C_{1+}. Contours of constant photon energy for silicon in the (110) plane. Contour lines are separated by 0.2 eV. Dashed lines are critical lines denoted by Greek letters. Stars are critical points, OCP. Circles are conduction-band ECP.

has a discontinuous first derivative. This nonanalytic character is unavoidable if one leaves the (110) plane, but for critical lines in the (110) plane it is computationally very helpful to use the reflection symmetry

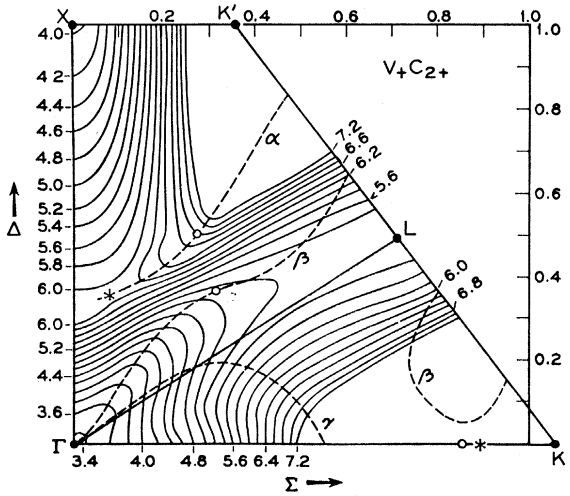

FIG. 12. Optical energy band; transition V_+ to C_{2+}. Contours of constant photon energy for silicon in the (110) plane. Contour lines are separated by 0.2 eV. Dashed lines are critical lines denoted by Greek letters. Stars are critical points, OCP. Circles are conduction-band ECP.

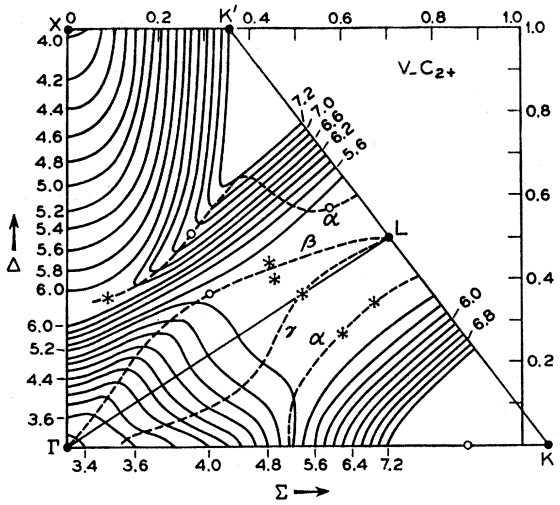

FIG. 13. Optical energy band; transition V_- to C_{2+}. Contours of constant photon energy for silicon in the (110) plane. Contour lines are separated by 0.2 eV. Dashed lines are critical lines denoted by Greek letters. Stars are critical points, OCP. Circles are conduction-band ECP.

and bypass the discontinuities introduced by an energy-ordering definition.

The energy bands studied are the two upper valence bands designated v_+ and v_- and the three lowest conduction bands designated c_{1+}, c_{2+}, and c_-. The $\pm$ subscript designates the reflection parity. Bands of the same parity are energy-ordered and the subscripts increase with increasing energy. We have also studied the six optical energy bands corresponding to transitions between the two upper valence bands and the three lowest conduction bands.

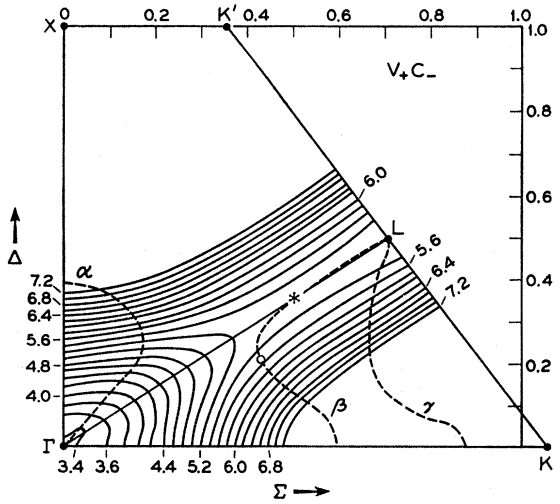

FIG. 14. Optical energy band; transition V_+ to C_-. Contours of constant photon energy for silicon in the (110) plane. Contour lines are separated by 0.2 eV. Dashed lines are critical lines denoted by Greek letters. Stars are critical points, OCP. Circles are conduction-band ECP.

We have computed energy contours for all these bands. The electron energy bands are shown in Figs. 5–9. The optical energy bands are shown in Figs. 10–15.

The energy interval between contour lines is 0.2 eV. The zero of energy is the top of the valence band. For a given band a total energy range of 3.8 eV was computed; hence many bands have a high- or low-energy cutoff beyond which calculations were not made.

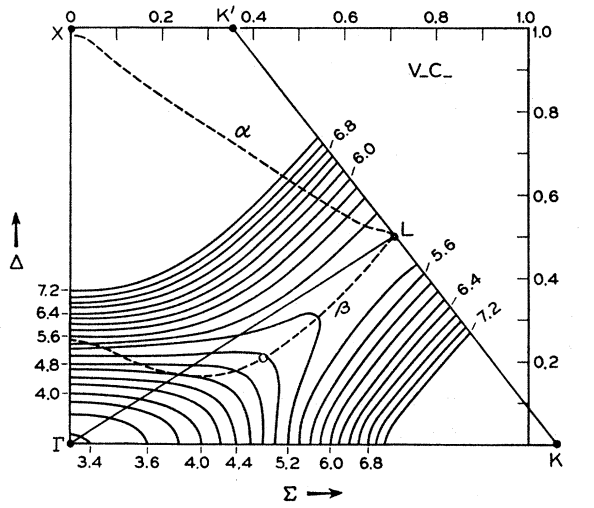

FIG. 15. Optical energy band; transition V_- to C_-. Contours of constant photon energy for silicon in the (110) plane. Contour lines are separated by 0.2 eV. Dashed lines are critical lines denoted by Greek letters. Stars are critical points, OCP. Circles are conduction-band ECP.

Energies, matrix elements, and first and second derivatives of energy with respect to $\mathbf{k}$ were computed on a rectangular grid. The line segment $\mathbf{k}=0$ to $\mathbf{k}=X$ ([100] direction) was subdivided into eight equal intervals; the line segment $\mathbf{k}=0$ to $\mathbf{k}=K$ ([110] direc-

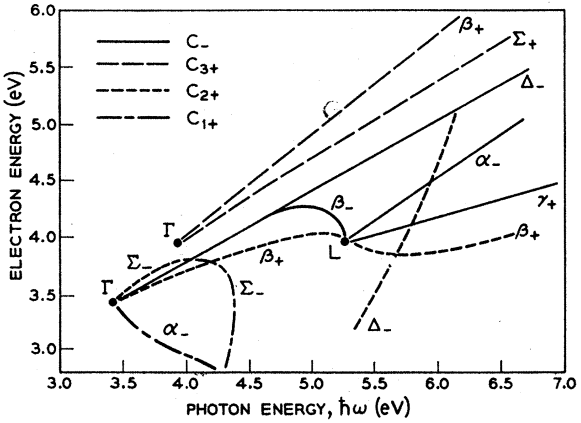

FIG. 16. E-ω images of critical lines in the (110) plane in silicon. Only the "strongest" lines have been selected. (Greek letter denotes critical lines as labeled in Figs. 10–15.) Final band indicated by code. Initial band indicated by subscript + or − on critical line designation. Γ and L SCP's indicated by heavy dots.

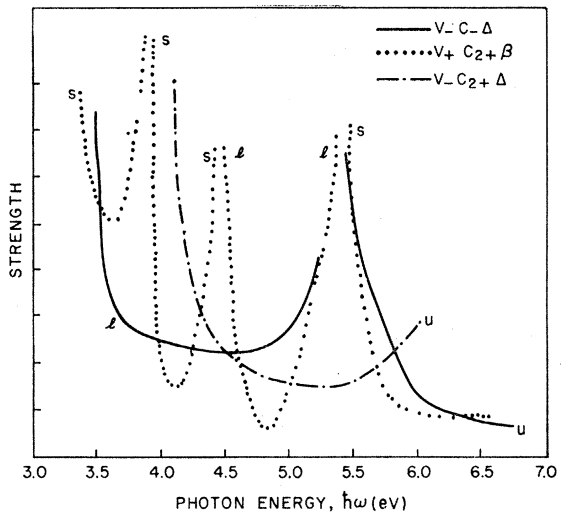

FIG. 17. Strength S_L versus photon energy of three of the strongest critical lines shown in Fig. 16. u, l, s indicates upper or lower extremum, or saddle-type critical point, CP_2.

tion) was subdivided into twelve equal intervals. For energy interpolations and other computations, the energy was taken to be given by a Taylor series to second order in $\Delta\mathbf{k}$, the distance to the closest mesh point. This approximation is not adequate in the vicinity of a nonanalytic point; e.g., Γ is nonanalytic for bands C_{1+} and C_{2+} which are degenerate at Γ. On the other hand, bands V_- and C_- are analytic in the (110) plane over the entire range computed since they do not contact other bands of the same reflection parity. However, quantities such as strengths of critical points and critical lines depend on the curvature normal to the (110) plane. Here, the analytic character out of the plane becomes important and our analytic approximation fails for many more points. For instance V_- and C_- are nonanalytic along the entire [100] and [111] directions when energies out of the (110) plane are considered.

Energy contours are required by symmetry to intersect perpendicularly the lines Δ and Σ. The same is required for the line Λ (Γ to L) where the bands are nondegenerate, as shown by band C_{1+} in Fig. 7. When the bands are degenerate along Λ, the symmetry requirement is that the slopes of the energy contours degenerate at Λ be equal and opposite relative to Λ. In short, reflection symmetry about Λ is required for the pair of bands but not for each band individually. This is shown by the degenerate pairs V_+, V_- and C_{2+}, C_-. Critical points, OCP and ECP, are designated by stars and circles, respectively.

The "flatness" of the "intermediate p band" C_{2+} shown in Fig. 8 is specially noteworthy. The flatness is most pronounced in the vicinity of the [111] direction. Calculations by Brust[7] and Kane[19] show a very strong peak in the density of states associated with this rather flat band.

In the optical energy graphs of Figs. 10–15 the critical lines CP_2 are shown dashed and are labeled with Greek letters α, β, γ. The symmetry lines Δ, Σ, and X-K' are necessarily critical lines due to symmetry. In Fig. 12 the three critical-line segments labeled α, β, and β are actually three parts of one continuous curve. This becomes apparent when the symmetry of the line $K'LK$ is considered. Points along this line which are related by inversion through L have equal energy. In particular, points K and K' have equal energy. In this case and elsewhere, parts α and β of the same line have been given different designations in order that the photon energy should be uniquely specified since we display the strength of critical lines as a function of photon energy.

The requirement that all ECP and OCP be intersected by one, and only one, critical line is seen to be satisfied in these figures. In addition the SCP are intersected by two or more critical lines. The point Γ has the largest number of critical lines because of its nonanalytic character.

In Fig. 14 the critical lines α and Δ provide an example of the fact that an ordinary critical line may intersect a symmetry critical line at a point other than an SCP.

In Fig. 16 we plot the E-ω images of some of the stronger critical lines displayed in Figs. 10–15. These are plots of electron energy versus photon energy taken along the critical lines. The SCP's Γ and L are seen to be important "foci" or "termini" for critical lines. Plots of this kind may serve to identify SCP's. The Γ point is easily distinguished even without a plot. Since Γ is the valence-band maximum, the Γ point lies on the 45° line $E=\hbar\omega$.

The strength S_L of the critical points CP_2 in Eqs. (23)–(25) have been calculated for three of the stronger critical lines and are plotted versus photon energy in Fig. 17. It is seen that the strength is a rapidly varying function of the photon energy. This may produce problems in plotting E-ω images experimentally since the structure may appear to fade into the background. The strength is large near SCP's where it will tend to infinity. The strength also tends to infinity wherever a change of type among s, l, u occurs.

The results of this paper have been briefly reported by Brust.[7] He has analyzed his calculated distributions in terms of "E-ω" plots and finds lines corresponding to $V_-C_{2+}\Sigma_-$ and $V_+C_{2+}\beta$ in Figs. 16 and 17. Higher resolution is required in the calculations in order to distinguish the less prominent details.

ACKNOWLEDGMENT

The author acknowledges useful conversations with D. Brust.

[19] E. O. Kane, Phys. Rev. **146**, 558 (1966).